
Likelihood-free inference with emulator networks

Jan-Matthis Lueckmann¹, Giacomo Bassetto¹,
Theofanis Karaletsos², Jakob H. Macke^{1,3,4}

¹ research center caesar, an associate of the Max Planck Society, Bonn, Germany

² Uber AI Labs, Uber Technologies, Inc., San Francisco, CA

³ Centre for Cognitive Science, Technische Universität Darmstadt, Germany

⁴ Neuroengineering, Department for Electrical and Computer Engineering,
Technical University of Munich, Germany

jan-matthis.lueckmann@caesar.de, giacomo.bassetto@caesar.de,
theofanis@uber.com, macke@tum.de

Abstract

Approximate Bayesian Computation (ABC) provides methods for Bayesian inference in simulation-based stochastic models which do not permit tractable likelihoods. We present a new ABC method which uses probabilistic neural *emulator* networks to learn synthetic likelihoods on simulated data – both ‘local’ emulators which approximate the likelihood for specific observed data, as well as ‘global’ ones which are applicable to a range of data. Simulations are chosen adaptively using an acquisition function which takes into account uncertainty about either the posterior distribution of interest, or the parameters of the emulator. Our approach does not rely on user-defined rejection thresholds or distance functions. We illustrate inference with emulator networks on synthetic examples and on a biophysical neuron model, and show that emulators allow accurate and efficient inference even on high-dimensional problems which are challenging for conventional ABC approaches.

1 Introduction

Many areas of science and engineering make extensive use of complex, stochastic numerical simulations which describe the structure and dynamics of the process being investigated [1]. These models are often derived from underlying physical or biological principles. Their parameters are therefore interpretable, often corresponding to measurable quantities, e.g., the density of ion-channels in the Hodgkin-Huxley equations in biophysical neuron models [2]. A key challenge in simulation-based science is linking such complex simulation models to empirical data.

Bayesian inference provides a general and powerful framework for identifying the set of model parameters which are consistent both with empirical data and prior knowledge. However, one of the key quantities required for statistical inference, the likelihood of observed data given parameters, $\mathcal{L}(\theta) = p(\mathbf{x}_o|\theta)$, is typically intractable for simulation-based models, rendering conventional statistical approaches inapplicable. Approximate Bayesian Computation (ABC) aims to close this gap by providing Bayesian inference algorithms that can be used with simulator models without requiring explicit likelihoods [3, 4, 5, 6, 7].

However, classical ABC-algorithms scale poorly to high-dimensional non-Gaussian data, and require *ad-hoc* choices which can significantly affect computational efficiency and accuracy: in sampling-based ABC algorithms [8, 4, 9], one repeatedly generates simulated data \mathbf{x}_n from different parameter θ_n , computes low-dimensional summary statistics $s(\mathbf{x}_n)$ and compares these summary statistics to those of the empirical data \mathbf{x}_o via a distance-measure $d(s(\mathbf{x}_n), s(\mathbf{x}_o))$. Based on some acceptance threshold ϵ , only samples which are sufficiently similar to the empirical data are accepted, i.e. whenever $d(s(\mathbf{x}_n), s(\mathbf{x}_o)) < \epsilon$. These approaches require choosing summary statistics (computed

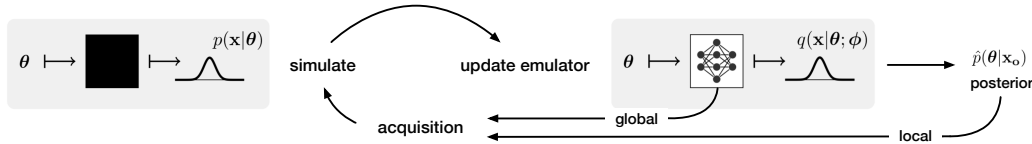


Figure 1: **Likelihood-free inference with emulator networks.** Our goal is to perform approximate Bayesian inference on ‘simulator’-models, i.e. models from which we can generate samples, but for which we can not evaluate likelihoods. Our approach is based on learning a tractable probabilistic emulator $q(\mathbf{x}|\theta; \phi)$ that approximates the simulator $p(\mathbf{x}|\theta)$. The emulator then serves as a synthetic likelihood to obtain an approximate posterior. To train the emulator using a low number of calls to the simulator, we use an active learning loop in which informative samples from the simulator are proposed selectively. The acquisition rule is either based on the current posterior estimate (if observed data \mathbf{x}_o is given, ‘local’ learning), or on our uncertainty about the weights of the emulator network (‘global learning’).

through $s(\cdot)$), a distance function $d(\cdot, \cdot)$ and a threshold ϵ , and these choices affect both computational efficiency and accuracy. In addition, these strategies lead to exact inference only if sufficient summary statistics are used, and in the limit of vanishing ϵ – i.e. in the limit in which virtually all samples would be rejected, leading to inherent trade-offs between sampling-efficiency and accuracy.

In *synthetic likelihood* approaches to ABC [10, 11, 12], one instead uses density estimation to approximate the likelihood $p(s(\mathbf{x}_o)|\theta)$ on summary statistics of simulated data. Typically, the summary statistics of simulated data for a given θ are assumed to be normally distributed, and the mean $\mu(\theta)$ and covariance $\Sigma(\theta)$ are estimated from repeated simulations. In order to exploit smoothness of likelihood functions across the parameter space, the use of Gaussian Processes (\mathcal{GPs}) has been proposed [13]. However, \mathcal{GPs} are not well suited for modelling multivariate heteroscedastic and correlated data. A recent proposal [14, 15] uses a \mathcal{GP} to approximate the distribution of the discrepancy $d(s(\mathbf{x}), s(\mathbf{x}_o))$ as a function of θ (rather than the data \mathbf{x} or summary statistics $s(\mathbf{x})$), and uses ideas from Bayesian Optimization to propose new parameters. While this approach can be very effective even with a small number of simulations, it still requires summary statistics, choice of a distance function $d(\cdot, \cdot)$, and relies on assuming a homoscedastic \mathcal{GP} .

The goal of this paper is to extend synthetic likelihood approaches to problems with high-dimensional observations and (potentially) non-Gaussian likelihoods, and without relying on user-defined distance functions. This opens the possibility of using likelihood free inference in settings in which it is difficult to choose good summary statistics. The core idea of our approach is to use neural networks as flexible conditional density estimators in synthetic likelihood approaches. Building on recent advances in learning probabilistic neural networks, we train an ensemble of networks which allows us to model uncertainty in the density estimator [16]. In order to keep the number of calls to the simulator low, we use active-learning strategies to adaptively propose new parameters to simulate from.

As our approach is inspired by classical work on emulating computer code with function approximators [17], we refer to these networks as ‘emulator networks’. We consider both approaches for learning ‘local’ emulators (i.e. for approximating the likelihood for particular, observed data \mathbf{x}_o), and ‘global’ emulators, which can then be rapidly applied to any newly observed data. We show that combining flexible, neural-network emulators with appropriately designed active-learning rules leads to likelihood-free inference algorithms which are efficient, flexible, and scale to high-dimensional observations, and which do not require user-defined distance functions.

2 Likelihood-free inference with emulator networks

Our goal is to obtain an approximation $\hat{p}(\theta|\mathbf{x}_o)$ of the true posterior $p(\theta|\mathbf{x}_o)$ of a black-box simulator model, i.e. a model from which we can draw samples, but for which both the likelihood function and gradients of the likelihood with respect to θ are intractable. To solve this task, we learn a synthetic likelihood function $\hat{\mathcal{L}}(\theta)$ by training a conditional density estimator on simulated data [18], and use active learning to propose parameters for subsequent simulations. The rationale for active learning is that simulations often are the dominant computational cost in ABC: Therefore, we want to keep the number of calls of the stochastic simulator as low as possible (Fig. 1).

The general approach is outlined in algorithm 1: Core to our approach is an emulator $q(\mathbf{x}|\boldsymbol{\theta}; \phi)$, a conditional density estimator with parameters ϕ that approximates the simulator $p(\mathbf{x}|\boldsymbol{\theta})$. Having collected an initial simulated dataset $\mathcal{D}^{N_{\text{initial}}}$, e.g. by repeatedly drawing from the prior $p(\boldsymbol{\theta})$ and simulating data, the emulator is trained. We actively select new locations $\boldsymbol{\theta}^*$ for which to simulate new data points $\mathcal{D}^* = \{(\boldsymbol{\theta}^*, \mathbf{x}^*)\}$ to append to the dataset, and subsequently update the emulator. The emulator therefore defines a synthetic likelihood function $\hat{\mathcal{L}}(\boldsymbol{\theta}; \phi) = q(\mathbf{x} = \mathbf{x}_o|\boldsymbol{\theta}; \phi)$ that we use to find an approximate posterior which is proportional to $\hat{\mathcal{L}}(\boldsymbol{\theta})p(\boldsymbol{\theta})$.

Thus, our approach requires (1) an emulator, i.e., a flexible conditional density estimator, (2) an approach for learning the emulator on simulated data and expressing our uncertainty about its parameters, (3) an acquisition rule for proposing new sampling locations, and (4) an inference procedure for obtaining the posterior distribution from the (synthetic) likelihood and the prior. We will describe these steps in the following.

2.1 Choice of emulator

We use neural network based emulators $q(\mathbf{x}|\boldsymbol{\theta}; \phi)$: parameters $\boldsymbol{\theta}$ are given as inputs to the network, and the network is trained to approximate $p(\mathbf{x}|\boldsymbol{\theta})$. In contrast to traditional synthetic likelihood approaches [10], we are not restricted to using a (multivariate) normal distribution to approximate the conditional density $p(\mathbf{x}|\boldsymbol{\theta})$. The output form of the emulator is chosen according to our knowledge regarding the conditional density of the simulator. In our second example application, we e.g. model $\mathbf{x}|\boldsymbol{\theta}$ as a binomial distribution over 8-bit integer pixel values, and in the third example we model a categorical distribution. If the noise model of the simulation process is unknown, flexible conditional density estimators such as conditional autoregressive models [19, 20] can be readily used in our approach.

2.2 Inference on the parameters of the emulator

We train probabilistic neural networks, i.e. we represent uncertainty about the parameters of the emulator network. We then use these uncertainties to guide the selection of sample points using active learning. In the Bayesian framework uncertainty is represented through the posterior distribution. Multiple approaches for estimating the posterior-distributions over neural-network parameters have been proposed, including MCMC methods (e.g. Stochastic Gradient MCMC) to draw samples from the full posterior [21, 22] and variational methods, which often use factorising posteriors [23], or normalizing flows [24]. Finally, deep ensemble approaches [16] represent predictive distributions through ensembles of networks which capture individual modes. They have the advantage of not requiring the choice of a functional form of the approximation, and are simple to set up.

Our approach can be applied with any method that represents uncertainty over parameters using samples of parameters, which could either come from a Bayesian posterior, or from deep ensembles. In our experiments, we use deep ensembles, as we found them to combine simplicity with good empirical performance. Instead of training a single emulator network and inferring its posterior distribution, we train an ensemble of M networks with parameters $\{\phi_m\}_{m=1}^M$. From here on, we treat ϕ_m as if they were samples from $p(\phi|\mathcal{D})$, the posterior over network parameters given data. (In practice, these samples will describe local maxima of the posterior.) The posterior-predictive distribution is given by

$$\hat{p}(\mathbf{x}|\boldsymbol{\theta}, \mathcal{D}) = \mathbb{E}_{\phi|\mathcal{D}}[q(\mathbf{x}|\boldsymbol{\theta}; \phi)] \approx \frac{1}{M} \sum_{m=1}^M q(\mathbf{x}|\boldsymbol{\theta}; \phi_m). \quad (1)$$

We note that the predictive distribution forms a mixture distribution over these samples, and consequently can be more expressive than the densities of the individual emulators.

Networks are trained supervised with data $\mathcal{D} = \{(\boldsymbol{\theta}_n, \mathbf{x}_n)\}_{n=1}^N$. During training, the parameters of the networks are optimized subject to the loss $-\sum_{m=1}^M \sum_{n=1}^N \log q(\mathbf{x}_n|\boldsymbol{\theta}_n; \phi_m)$ w.r.t. ϕ (a proper scoring rule as discussed in [16]). Networks in the ensemble are initialized differently, and data points are randomly shuffled during training (different order per network). [16] also showed that adversarial training procedure are beneficial on some datasets, but we did not pursue this direction here.

Algorithm 1: ABC via active learning to learn a synthetic likelihood

Input : $p(\boldsymbol{\theta}), p(\mathbf{x}|\boldsymbol{\theta}), \mathbf{x}_o$ // prior, stochastic simulator, observed data
Output : $\hat{p}(\boldsymbol{\theta}|\mathbf{x}_o)$ // approximate posterior

1 $\mathcal{D} \leftarrow \mathcal{D}^{N_{\text{initial}}} = \{(\boldsymbol{\theta}_n, \mathbf{x}_n)\}_{n=1}^{N_{\text{initial}}} \sim p(\mathbf{x}, \boldsymbol{\theta})$ // $\boldsymbol{\theta}_n \sim p(\boldsymbol{\theta}), \mathbf{x}_n \sim p(\mathbf{x}|\boldsymbol{\theta}_n)$

2 **do**

3 Train emulator $q(\mathbf{x}|\boldsymbol{\theta}; \phi)$ on \mathcal{D}

4 Find $\boldsymbol{\theta}^*$ as the maximum of an acquisition function

5 Acquire new data point $\mathcal{D}^* = \{(\boldsymbol{\theta}^*, \mathbf{x}^*)\}$ by simulating for $\boldsymbol{\theta}^*$ // $\mathbf{x}^*|\boldsymbol{\theta}^* \sim p(\mathbf{x}|\boldsymbol{\theta}^*)$

6 $\mathcal{D} \leftarrow \mathcal{D} \cup \mathcal{D}^*$

7 **while** *not converged*

8 Find $\hat{p}(\boldsymbol{\theta}|\mathbf{x}_o)$ using the synthetic likelihood $\hat{\mathcal{L}}(\boldsymbol{\theta}) = q(\mathbf{x}_o|\boldsymbol{\theta}; \phi)$

2.3 Acquisition rules

Key to our approach is active learning to selectively acquire new samples. We distinguish between two scenarios: In the first, we have particular observed data \mathbf{x}_o available, and train a ‘local’ emulator for inference. Approximating the likelihood near \mathbf{x}_o is an easier goal than globally approximating the simulator for all possible \mathbf{x} , as $q(\mathbf{x}|\boldsymbol{\theta}; \phi)$ does not need to be accurate across all \mathbf{x} (we only want to use it as a likelihood function for which we evaluate it at $\mathbf{x} = \mathbf{x}_o$).

However, as a downside, this approach requires learning a new emulator for each new observed data \mathbf{x}_o . Therefore, we also consider a second scenario, in which we learn a ‘global’ emulator that is valid for a range of data. Learning a global emulator is more challenging and may potentially require more flexible density estimators. However, once the emulator is learned, we can readily approximate the likelihood for *any* $\mathbf{x} = \mathbf{x}_o$, therefore amortizing the cost of learning the emulator. The two scenarios call for different acquisition functions for proposing new samples, which we will discuss next.

2.3.1 Learning a local emulator

With given \mathbf{x}_o , we want to learn a local emulator that allows us to derive a good approximation to the (unnormalized) posterior

$$\tilde{p}(\boldsymbol{\theta}|\mathbf{x}_o) \propto \mathbb{E}_{\phi|\mathcal{D}} [q(\mathbf{x} = \mathbf{x}_o|\boldsymbol{\theta}; \phi)] p(\boldsymbol{\theta}). \quad (2)$$

As we are interested in increasing our certainty about the posterior, we target its variance, $\mathbb{V}_{\phi|\mathcal{D}}[\tilde{p}(\boldsymbol{\theta}|\mathbf{x}_o, \phi)]$, where $\mathbb{V}_{\phi|\mathcal{D}}$ denotes that we take the variance with respect to the posterior over network weights given data \mathcal{D} . Thus, we use an acquisition rule which targets the region of maximum variance in the predicted (unnormalized) posterior,

$$\begin{aligned} \boldsymbol{\theta}^* &= \arg \max_{\boldsymbol{\theta}} \mathbb{V}_{\phi|\mathcal{D}}[\tilde{p}(\boldsymbol{\theta}|\mathbf{x}_o, \phi)] \\ &= \arg \max_{\boldsymbol{\theta}} p(\boldsymbol{\theta})^2 \mathbb{V}_{\phi|\mathcal{D}}[\hat{\mathcal{L}}(\boldsymbol{\theta})] \\ &= \arg \max_{\boldsymbol{\theta}} \log p(\boldsymbol{\theta}) + \log \sqrt{\mathbb{V}_{\phi|\mathcal{D}}[\hat{\mathcal{L}}(\boldsymbol{\theta})]}. \end{aligned} \quad (3)$$

For all practical purposes, we approximate $\mathbb{V}_{\phi|\mathcal{D}}$ with the sample variance taken across ϕ_m drawn from the posterior over networks. We refer to this rule as the *MaxVar* rule.

In practice, we optimize this acquisition rule by using gradient descent, making use of automatic differentiation to take gradients with respect to $\boldsymbol{\theta}$ through the synthetic likelihood function specified by the emulator. *MaxVar* is one possible rule to learn a local emulator. More sophisticated rule could take into account past or potential future acquisitions, and we see this as a promising avenue for future work.

2.3.2 Learning a global emulator

In the second scenario we want to learn a global emulator. A global emulator may be used to do inference once \mathbf{x}_o becomes available. Here, the goal for active learning is to bring the emulator

$q(\mathbf{x}|\boldsymbol{\theta}; \phi)$ close to the simulator $p(\mathbf{x}|\boldsymbol{\theta})$ for all $\boldsymbol{\theta}$ s using as few runs of the simulator as possible. We use a rule based on information theory from the active learning literature [25, 26, 27]. We will refer to the rule

$$\begin{aligned} \boldsymbol{\theta}^* &= \arg \max_{\boldsymbol{\theta}} \mathbb{I}[\mathbf{x}, \phi|\boldsymbol{\theta}, \mathcal{D}] \\ &= \arg \max_{\boldsymbol{\theta}} \underbrace{\mathbb{H}[\mathbf{x}|\boldsymbol{\theta}, \mathcal{D}]}_{\text{entropy}} - \underbrace{\mathbb{E}_{\phi|\mathcal{D}}[\mathbb{H}[\mathbf{x}|\boldsymbol{\theta}, \phi]]}_{\text{expected conditional entropy}} \end{aligned} \quad (4)$$

as the maximum mutual information rule (*MaxInf*).

The first term is the entropy of the data under the posterior-predictive distribution implied by the emulator:

$$\mathbb{H}[\mathbf{x}|\boldsymbol{\theta}, \mathcal{D}] = - \int \hat{p}(\mathbf{x}|\boldsymbol{\theta}, \mathcal{D}) \ln \hat{p}(\mathbf{x}|\boldsymbol{\theta}, \mathcal{D}) d\mathbf{x}, \quad (5)$$

where $\hat{p}(\mathbf{x}|\boldsymbol{\theta}, \mathcal{D})$ is obtained by marginalizing out the emulator’s parameters w.r.t. $p(\phi|\mathcal{D})$:

$$\hat{p}(\mathbf{x}|\boldsymbol{\theta}, \mathcal{D}) = \int p(\mathbf{x}|\boldsymbol{\theta}, \phi) p(\phi|\mathcal{D}) d\phi. \quad (6)$$

The expected conditional entropy, $\mathbb{E}_{\phi|\mathcal{D}}[\mathbb{H}[\mathbf{x}|\boldsymbol{\theta}, \phi]]$, is the average entropy of the output \mathbf{x} for a particular choice of inputs $\boldsymbol{\theta}$ and emulator parameters ϕ , under the posterior distribution of emulator parameters $p(\phi|\mathcal{D})$. Again, we treat ensemble members ϕ_m as if they were draws from $p(\phi|\mathcal{D})$. Housley et al. [25] refer to this rule as Bayesian Active Learning by Disagreement (BALD): we query parameters $\boldsymbol{\theta}$ where the posterior predictive is very uncertain about the output (entropy is high), but the emulator, conditioned on the value of its parameters ϕ , is on average quite certain about the model output (conditional entropy low on average).

For many distributions closed-form expressions of $\mathbb{H}[\mathbf{x}|\boldsymbol{\theta}, \phi]$ are available, but this is in general not true for the entropy of the marginal predictive distribution $\hat{p}(\mathbf{x}|\boldsymbol{\theta}, \mathcal{D})$. To overcome this problem, we derived an upper-bound approximation to the entropy term based on the law of total variance: if we characterize the marginal distribution only in terms of its (co)variance $\Sigma_{\mathcal{D}}(\boldsymbol{\theta})$, then $\mathbb{H}[\mathbf{x}|\boldsymbol{\theta}, \mathcal{D}] \leq \frac{1}{2} \ln [(2\pi e)^N |(\Sigma_{\mathcal{D}}(\boldsymbol{\theta}))|]$. Using the law of total (co)variance, we get

$$\Sigma_{\mathcal{D}}(\boldsymbol{\theta}|\mathcal{D}) = \text{Cov}[\mathbf{x}|\boldsymbol{\theta}] = \mathbb{E}_{\phi|\mathcal{D}}[\text{Cov}[\mathbf{x}|\boldsymbol{\theta}, \phi]] + \text{Cov}_{\phi|\mathcal{D}}[\mathbb{E}[\mathbf{x}|\boldsymbol{\theta}, \phi]], \quad (7)$$

where all expectations can be approximated by samples drawn from $p(\phi|\mathcal{D})$.

2.4 Deriving the posterior distribution from the emulator

Once we have learned the emulator, we use Hamiltonian Monte Carlo (HMC, [28]) to draw samples from our approximate posterior, using the emulator-based synthetic likelihood. We generate samples of $\boldsymbol{\theta}$ drawn from the distribution

$$\tilde{p}(\boldsymbol{\theta}|\mathbf{x}_o) = \mathbb{E}_{\phi|\mathcal{D}}[q(\mathbf{x}_o|\boldsymbol{\theta})] p(\boldsymbol{\theta}). \quad (8)$$

In practice, we sample $\boldsymbol{\theta}$ from each ensemble member individually and use the union of all samples as a draw from the approximate posterior. We could also obtain the posterior through variational inference, but here prefer to retain full flexibility in the shape of the inferred posterior.

3 Results

We demonstrate likelihood-free inference with emulator networks on three examples: first, we show that emulators are competitive with state-of-the-art on an example with Gaussian observations; second, we demonstrate the ability of emulators to work with high-dimensional, raw observations while learning to amortize the simulator; third, we show an application to a ‘real-world’ simulator and identify the posterior over biophysical parameters of a Hodgkin-Huxley neuron model [29].

3.1 A low-dimensional example: Simulator with Gaussian observations

We first demonstrate emulator networks on a non-linear model between parameters and data, corrupted by additive Gaussian observation noise: data is generated according to $\mathbf{x}_i \sim \mathcal{N}(\cdot|f(\boldsymbol{\theta}), \boldsymbol{\Sigma})$, $i = 1 \dots n$, where $f(\boldsymbol{\theta})$ is cubic in $\boldsymbol{\theta}$, $\boldsymbol{\Sigma}$ is fixed, and $\boldsymbol{\theta}$ is distributed uniformly (see Appendix A for

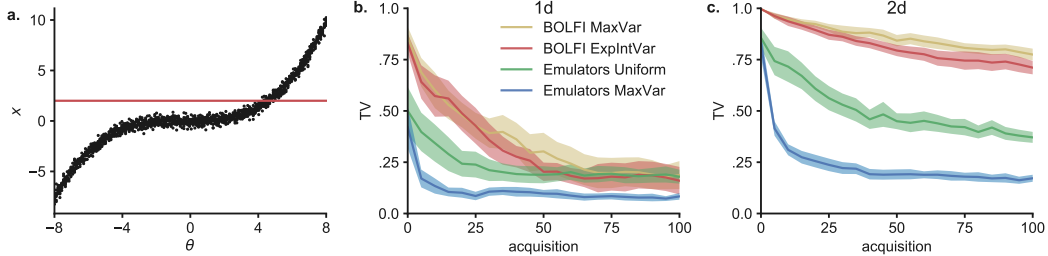


Figure 2: **Inference on simulator with Gaussian noise.** **a.** Data is generated from $\mathbf{x} \sim \mathcal{N}(\mathbf{x}|f(\boldsymbol{\theta}), \boldsymbol{\Sigma})$, i.e. using a Gaussian conditional density where the relationship between parameter $\boldsymbol{\theta}$ and mean is a non-linear function $f(\cdot)$. We illustrate posterior inference $p(\boldsymbol{\theta}|\mathbf{x}_o)$ given $\mathbf{x}_o = 2$ (red line). **b.** In 1-D, emulator-based inference (see text for details) with the *MaxVar* acquisition function leads to faster convergence to the true posterior than uniform sampling, or BOLFI. Lines are means and SEMs from 20 runs. **c.** Same problem as in **b**, but \mathbf{x} and $\boldsymbol{\theta} \in \mathbb{R}^2$ and the non-linearity is applied point-wise.

complete specification of this example). The goal is to approximate the posterior $p(\boldsymbol{\theta}|\bar{\mathbf{x}}_o)$ from the smallest possible number of draws from the generative model (Fig. 2a). For the emulator, we use a neural network with one hidden layer consisting of 10 tanh units, whose outputs are combined to produce the mean and the variance of $p(\mathbf{x}|\boldsymbol{\theta})$.

We will compare our method to BOLFI (Bayesian Optimization for Likelihood-free Inference, [15]), an ABC method which – given a user-specified discrepancy measure – learns a \mathcal{GP} that models the distribution of discrepancies between summary statistics of \mathbf{x} and \mathbf{x}_o . Järvenpää et al. [14] proposed multiple acquisition rules for BOLFI. The most principled (but also most costly) rule minimizes the expected integrated variance (*ExpIntVar*) of the approximate posterior after acquiring new data [30, 14]. On a number of problems, BOLFI is state-of-the-art for simulation-efficient likelihood-free inference, and substantially more efficient than classical rejection-based methods (such as rejection-ABC[8], MCMC-ABC[4], SMC-ABC[9]).

We use the total variation (TV) between true and approximate posterior (evaluated using numerical integration) to quantify performance. We find that emulators with *MaxVar* sampling work better than uniform sampling (Fig. 2b). Both BOLFI rules (*ExpIntVar* and *MaxVar*) exhibit very similar performance, but require higher number of simulations than emulators to reach low TV values. On a 2-dimensional version of the problem, the qualitative ordering is the same, but the differences between methods are greater (Fig. 2c). We did additional runs of BOLFI *MaxVar* to confirm that it eventually converges towards the correct posterior. However, convergence is slow and the quality of the inferred posterior depends strongly on the choice of the threshold parameter used in BOLFI (see Appendix E).

3.2 High-dimensional observations: Inferring the location and contrast of a blob

In this example, we show that our method can be applied to estimation problems with high-dimensional observations without having to resort to using summary statistics[31]. We model the rendering of a blob on a 2D image, and learn a ‘global’ emulator for the forward model. The forward model takes as inputs three parameters (x_{off} , y_{off} and γ) – which encode horizontal and vertical displacement, and contrast of the blob – and returns per-pixels activation probabilities p_{ij} . The value of each pixel v_{ij} is then generated according to a binomial distribution with total count 255 (8-bits gray-scale image) and probability p_{ij} , resulting in a 32×32 pixel image (Fig. 3a; see Appendix B for further details). In this application, we use a multi-layer neural network (see Appendix B for details) whose output is, for each pixel, the mean parameter of the binomial distribution.

Using the *MaxInf* rule to acquire new test points in parameters space results in faster learning of the emulator, compared to uniform random acquisitions (Fig. 3b). Eventually, both rules converge towards the log-likelihood (LL) of the held-out testset, indicating successful global emulation of the forward model. Next, we used emulator networks for inference. Images in Fig. 3a were used as observations: Images generated from parameters sampled from the posterior distribution are in

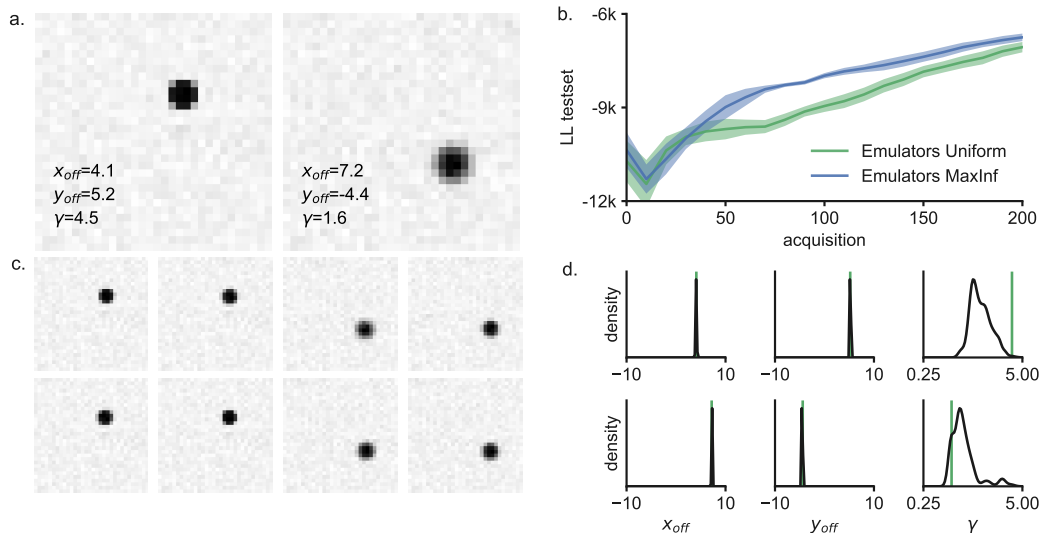


Figure 3: **Inferring location and scale of a blob** **a.** Illustration of the model on two sample images. Parameters are the spatial position and contrast of the blob. **b.** Acquiring samples using the *MaxInf* rule yield to faster learning of $p(\mathbf{x}|\boldsymbol{\theta})$ than with samples acquired uniformly in the parameter space. Performances are reported as log-likelihood of held-out test data under the emulators learned in the two different scenarios. **c.** Sample images drawn from posterior. **d.** Marginals of posterior over the three parameters, ground-truth parameters marked in green.

good agreement with the observations (Fig. 3c), indicating that the posterior was tightly constrained. Ground truth parameters are within the marginals of the posterior (Fig. 3d).

3.3 Hodgkin-Huxley model

As an example of a scientific application, we use the Hodgkin-Huxley model [29, 32] which describes the evolution of membrane potential in neurons (Fig. 4a). Fitting single- and multi-compartment Hodgkin-Huxley models to neurophysiological data is a central problem in neuroscience, and typically addressed using non-Bayesian approaches based on evolutionary optimization [33, 34]. In contrast to the previous examples, we do not model the raw data \mathbf{x} , but summary features derived from them. While this is often done out of necessity, calculating the posterior relative to summary statistics can often be of scientific interest [35]. This is indeed the case when fitting parameters of biophysical models in neuroscience, which is typically performed carefully chosen summary statistics which represent data-properties of particular interest [33, 34].

Here, we chose to model the number of action potentials (or spikes) in response to a step-current input, and we are interested in the set of parameters that are consistent with the observed number of action potentials. The conditional density of the emulator networks becomes a categorical distribution with 6 classes, modelling the probabilities of exactly 0, 1, \dots 4 spikes, and 5 or more spikes (which never occurred under the parameter ranges we explored). Model parameters $\boldsymbol{\theta}$ are the ion-channel conductances \bar{g}_{Na} and \bar{g}_K , controlling the shape and frequency of the spikes (further details in Appendix C).

We trained emulator networks using *MaxInf* to infer the posterior probabilities over $\boldsymbol{\theta}$ generating a given number of observed spikes – the acquisition surface is shown in Appendix F. Resulting posterior distributions are shown in Fig. 4b, along with a posterior predictive check showing that the mapping between parameters and summary features was learned correctly.

4 Discussion

We presented an approach for performing statistical inference on simulation-based models which do not permit tractable likelihood. Our approach is based on learning an ‘emulator network’, i.e. a probabilistic model that is consistent with the simulation, and for which likelihoods are tractable.

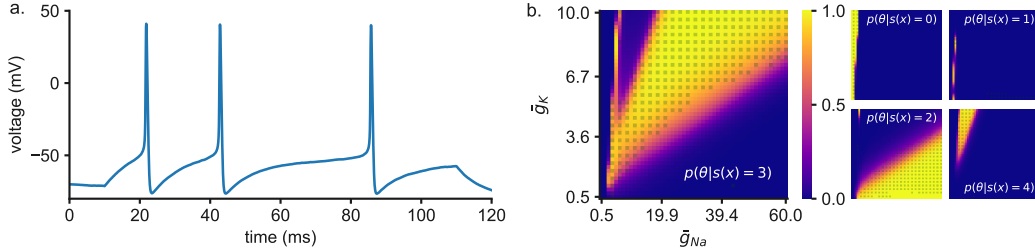


Figure 4: **Hodgkin-Huxley model** **a.** An example trace obtained from the system of differential equations describing the model. **b.** Posterior inferred for number of spikes, including predictive check. The largest panel shows the posterior given three spikes. We ran simulations on a regular grid over the parameter space. We overlay a transparent square on top of the posterior where simulations produced 3 spikes (and no such square otherwise). This is done analogously for the other panels.

The likelihoods of the emulator can then be plugged into any Bayesian inference approach (as in synthetic likelihood approaches [10, 11, 36]) to calculate the posterior. Active learning can be used to adaptively suggest new samples to reduce the number of calls to the simulator. We discussed two acquisition functions for learning ‘local’ and ‘global’ emulators, we showed that our approach scales to high-d observation spaces, does not require user-defined distance functions or acceptance thresholds, and is not limited to Gaussian observations – all of which are challenging for conventional ABC approaches.

Our approach uses density estimation to approximate the likelihood. A complementary use of density-estimation in ABC is to directly target the posterior distribution [6, 37, 38, 39]. This approach can be very useful – however, one advantage of likelihood-based approaches is that they allow one to apply the same synthetic likelihood to multiple priors (without having to retrain), or to pool information from multiple observations (by multiplying the corresponding synthetic likelihoods). More technically, posterior density estimation gives less flexibility in proposing samples – in order to yield the correct posterior, samples have to be drawn from the prior, or approaches such as importance-weighting [37] or other post-hoc corrections [6] have to be applied.

There are multiple ways in which our approach can be improved further: First, one could use alternative, and more expressive neural-network based density estimators, e.g. ones based on normalizing flows [20]¹. Second, one could use Bayesian posterior estimation (rather than ensembles) to capture parameter uncertainty, and/or use variational inference (rather than HMC-ABC) to derive an estimate of the posterior from the synthetic likelihood provided by the emulator. Third, we presented two acquisition functions (one for local and one for global estimation) – it is likely that the approach can be made more simulation-efficient by using different, and more sophisticated acquisition functions. In particular, our *MaxVar* rule targets the parameters with maximal uncertainty, but does not try to predict whether that uncertainty will be effectively reduced. However, evaluating acquisition functions like *ExpIntVar* can be computationally expensive – it will be useful to develop approaches which are sensitive to the relative cost of simulations and proposals, and adaptively adjust the acquisition function used.

Numerical simulations make it possible to model complex phenomena from first principles, and are indispensable tools in many fields in engineering and science. The advent of powerful approaches for statistical inference in simulation-based models [7] is opening up exciting opportunities for closing the gap between mechanistic, simulation-based and statistical approaches to modelling complex systems. Our Bayesian methodology based on emulators provides a fast, effective surrogate model for the intractable likelihood implied by the simulator, and the active-learning based rules lead to bounded-rational decisions about which simulations to run. In combination, they form a rigorous and resource-efficient basis for data analysis with simulators in the loop.

¹In fact, Papamakarios, Sterratt, and Murray [40], concurrently and independently proposed this approach for likelihood-free inference: They use Masked Autoregressive Flows as synthetic likelihoods and demonstrate state-of-the-art performance compared to methods that directly target the posterior. Like our approach, the density estimator is trained on sequentially chosen simulations. Rather than using acquisition functions that take into account uncertainty to guide sampling, they draw samples from the current estimate of the posterior. Their approach corresponds to an alternative way of learning a local emulator.

Acknowledgements

We thank Marcel Nonnenmacher and Pedro J. Gonçalves for discussions, and help with simulation of the Hodgkin-Huxley model. We thank David Greenberg and all members of the Neural Systems Analysis group for comments on the manuscript.

This work was supported by SFB 1089 (University of Bonn), SFB 1233 (University of Tübingen), and SPP 2041 of the German Research Foundation (DFG) to JHM, as well as by the caesar foundation.

References

- [1] G Karabatsos and F Leisen. An Approximate Likelihood Perspective on ABC Methods. *arXiv:1708.05341*, 2017.
- [2] W Gerstner, H Sprekeler, and G Deco. Theory and Simulation in Neuroscience. *Science*, 338(6103), 2012.
- [3] M Beaumont, W Zhang, and D J Balding. Approximate bayesian computation in population genetics. *Genetics*, 162(4), 2002.
- [4] P Marjoram, J Molitor, V Plagnol, and S Tavaré. Markov chain monte carlo without likelihoods. *Proceedings of the National Academy of Sciences*, 100(26), 2003.
- [5] M G B Blum and O François. Non-linear regression models for approximate bayesian computation. *Statistics and Computing*, 20(1), 2010.
- [6] G Papamakarios and I Murray. Fast epsilon-free inference of simulation models with bayesian conditional density estimation. In *Advances in Neural Information Processing Systems*, 2017.
- [7] J Brehmer, K Cranmer, G Louppe, and J Pavez. Constraining effective field theories with machine learning. *arXiv:1805.00013*, 2018.
- [8] J K Pritchard, M T Seielstad, A Perez-Lezaun, and M W Feldman. Population growth of human y chromosomes: a study of y chromosome microsatellites. *Mol Biol Evol*, 16(12), 1999.
- [9] S A Sisson, Y Fan, and M M Tanaka. Sequential Monte Carlo without likelihoods. *Proceedings of the National Academy of Sciences*, 104(6), 2007.
- [10] S N Wood. Statistical inference for noisy nonlinear ecological dynamic systems. *Nature*, 466(7310), 2010.
- [11] V M H Ong, D J Nott, M Tran, S A Sisson, and C C Drovandi. Variational bayes with synthetic likelihood. *arXiv:1608.03069*, 2016.
- [12] L F Price, C C Drovandi, A Lee, and D J Nott. Bayesian Synthetic Likelihood. *Journal of Computational and Graphical Statistics*, 27(1), 2018.
- [13] E Meeds, M Welling, et al. Gps-abc: Gaussian process surrogate approximate bayesian computation. *UAI*, 2014.
- [14] M Järvenpää, M U Gutmann, A Pleska, Aki, V, and P Marttinen. Efficient acquisition rules for model-based approximate Bayesian computation. *arXiv:1704.00520v2*, 2017.
- [15] M U Gutmann and J Corander. Bayesian Optimization for Likelihood-Free Inference of Simulator-Based Statistical Models. *Journal of Machine Learning Research*, 17(125), 2016.
- [16] B Lakshminarayanan, A Pritzel, and C Blundell. Simple and Scalable Predictive Uncertainty Estimation using Deep Ensembles. *arXiv:1612.01474*, 2016.
- [17] M C Kennedy and A O’Hagan. Bayesian calibration of computer models. *Journal of the Royal Statistical Society: Series B (Statistical Methodology)*, 63(3), 2002.
- [18] V Jethava and Dubhashi D P. Gans for LIFE: generative adversarial networks for likelihood free inference. *arXiv:1711.11139*, 2017.

- [19] A van den Oord, N Kalchbrenner, and K Kavukcuoglu. Pixel recurrent neural networks. *arXiv:1601.06759*, 2016.
- [20] G Papamakarios, T Pavlakou, and I Murray. Masked Autoregressive Flow for Density Estimation. *arXiv:1705.07057*, 2017.
- [21] M Welling and Y W Teh. Bayesian Learning via Stochastic Gradient Langevin Dynamics. In *Proceedings of the 28th International Conference on International Conference on Machine Learning*. Omnipress, 2011.
- [22] T Chen, E B Fox, and C Guestrin. Stochastic Gradient Hamiltonian Monte Carlo. *arXiv:1402.4102*, 2014.
- [23] C Blundell, J Cornebise, K Kavukcuoglu, and D Wierstra. Weight Uncertainty in Neural Networks. *arXiv:1505.05424*, 2015.
- [24] C Louizos and M Welling. Multiplicative normalizing flows for variational bayesian neural networks. *arXiv:1703.01961*, 2017.
- [25] N Hounsby, F Huszar, Z Ghahramani, and M Lengyel. Bayesian active learning for classification and preference learning. *arXiv:1112.5745*, 2011.
- [26] Y Gal, R Islam, and Z Ghahramani. Deep bayesian active learning with image data. *arXiv:1703.02910*, 2017.
- [27] S Depeweg, J M Hernández-Lobato, F Doshi-Velez, and S Udfluft. Decomposition of uncertainty for active learning and reliable reinforcement learning in stochastic systems. *arXiv:1710.07283*, 2017.
- [28] R M Neal. MCMC using Hamiltonian dynamics. *Handbook of Markov Chain Monte Carlo*, 54: 113–162, 2010.
- [29] M Pospischil, M Toledo-Rodriguez, C Monier, Z Piwkowska, T Bal, Y Frégnac, H Markram, and A Destexhe. Minimal hodgkin-huxley type models for different classes of cortical and thalamic neurons. *Biological Cybernetics*, 99(4-5), 2008.
- [30] P Hennig, M A Osborne, and M Girolami. Probabilistic numerics and uncertainty in computations. *Proceedings of the Royal Society of London A: Mathematical, Physical and Engineering Sciences*, 471(2179), 2015.
- [31] D J Nott, V MH. Ong, Y Fan, and S A Sisson. High-dimensional ABC. *arXiv:1802.09725*, 2018.
- [32] A L Hodgkin and Huxley A F. A quantitative description of membrane current and its application to conduction and excitation in nerve. *The Journal of Physiology*, 117(4), 1952.
- [33] S Druckmann, Y Banitt, A Gidon, F Schürmann, H Markram, and I Segev. A novel multiple objective optimization framework for constraining conductance-based neuron models by experimental data. *Frontiers in Neuroscience*, 1, 2007.
- [34] W Van Geit, M Gevaert, G Chindemi, C Rössert, JD Courcol, E B Muller, F Schürmann, I Segev, and H Markram. Bluepyopt: Leveraging open source software and cloud infrastructure to optimise model parameters in neuroscience. *Frontiers in Neuroinformatics*, 10, 2016.
- [35] C Andrieu, S Barthelme, M Chopin, J Cornebise, A Doucet, M Girolami, I Kosmidis, A Jasra, A Lee, J M Marin, C P Pudlo, P Robert, M Sedki, and S S Singh. Some discussions of d. fearhead and d. prangle’s read paper "constructing summary statistics for approximate bayesian computation: semi-automatic approximate bayesian computation. *arXiv:1201.1314*, 2012.
- [36] V MH Ong, D J Nott, and M S Smith. Gaussian variational approximation with a factor covariance structure. *arXiv:1701.03208*, 2017.
- [37] JM Lueckmann, P J Goncalves, G Bassetto, K Öcal, M Nonnenmacher, and J H Macke. Flexible statistical inference for mechanistic models of neural dynamics. In *Advances in Neural Information Processing Systems 30*. Curran Associates, Inc., 2018.

- [38] T A Le, A G Baydin, R Zinkov, and F D Wood. Using synthetic data to train neural networks is model-based reasoning. *arXiv:1703.00868*, 2017.
- [39] R Izbicki, A B Lee, and T Pospisil. Abc-cde: Towards approximate bayesian computation with complex high-dimensional data and limited simulations. *arXiv:1805.05480*, 2018.
- [40] George Papamakarios, David C. Sterratt, and Iain Murray. Sequential Neural Likelihood: Fast Likelihood-free Inference with Autoregressive Flows. *arXiv:1805.07226*, 2018.

Appendix

A Gaussian simulator

A.1 Model

Data is generated independently according to $\mathbf{x}_i \sim \mathcal{N}(\cdot|f(\boldsymbol{\theta}), \boldsymbol{\Sigma})$, $i = 1 \dots n$, where $n = 10$, $f(\boldsymbol{\theta}) = (1.5 \boldsymbol{\theta} + 0.5)^3/200$, $\boldsymbol{\Sigma}_{ii} = 0.1$, $\boldsymbol{\Sigma}_{ij} = 0$ for $i \neq j$, $\bar{\mathbf{x}}_o = \frac{1}{n} \sum_i^n \bar{\mathbf{x}}_o^{(i)} = \mathbf{2}$, and $\boldsymbol{\theta}$ is distributed uniformly in $[-8, 8]^p$ where p is the dimensionality of the problem.

This problem is inspired by the Gaussian example studied in [1], where f was chosen as $f(\boldsymbol{\theta}) = \boldsymbol{\theta}$. We introduce a nonlinearity in f , since our method with uniform acquisitions would otherwise trivially generalize across the space – we observed that a neural network with the right amount of ReLU units can learn the linear mapping perfectly, independently of where the training samples are acquired.

A.2 Evaluation

We evaluate our method and BOLFI [1] on this problem in 1D and 2D. In 1D, algorithms start with $t_0 = 10$ initial samples, in 2D with $t_0 = 25$, and make 100 acquisitions after each of which we evaluate how well the ground truth posterior is recovered.

As performance metric, we calculate total variation (TV) between $\hat{p}(\boldsymbol{\theta}|\mathbf{x}_o)$ and $p(\boldsymbol{\theta}|\mathbf{x}_o)$, defined as

$$\frac{1}{2} \int \left| \hat{p}(\boldsymbol{\theta}|\mathbf{x}_o) - p(\boldsymbol{\theta}|\mathbf{x}_o) \right| d\boldsymbol{\theta}.$$

A.3 Network architecture and training

Emulator networks model a normal distribution as output, so that the outputs of the network parametrise mean and covariance (Cholesky factor of the covariance matrix). Neural networks have one hidden layer consisting of 10 tanh units. We train an ensemble of $M = 50$ networks using Adam [2] with default parameters ($\beta_1 = 0.9, \beta_2 = 0.999$) for SGD, and a learning rate of 0.01.

A.4 BOLFI

BOLFI requires choice of a distance function: We use the the Mahalanobis distance

$$\Delta_{\boldsymbol{\theta}} = ((\bar{\mathbf{x}} - \bar{\mathbf{x}}_o)^T \boldsymbol{\Sigma}^{-1} (\bar{\mathbf{x}} - \bar{\mathbf{x}}_o))^{1/2},$$

in line with the distance function used for the Gaussian example studied in [1]. We use the implementation provided by the authors [3].

References

- [1] M Järvenpää, M U Gutmann, A Pleska, V Aki, and P Marttinen. Efficient acquisition rules for model-based approximate Bayesian computation. *arXiv:1704.00520v2*, 2017.
- [2] D Kingma and J Ba. Adam: A Method for Stochastic Optimization. In *ICLR*, 2015.
- [3] J Lintusaari, H Vuollekoski, A Kangasrääsio, K, Skytén, M Järvenpää, M Gutmann, A Vehtari, J Corander, and S Kaski. ELFI: Engine for Likelihood Free Inference. *arXiv:1708.00707*, 2017.

B Image generation

B.1 Model

Images are generated according to:

$$\begin{aligned} I_{xy} &\sim \text{Bin}(\cdot|255, p_{xy}) \\ p_{xy} &= 0.9 - 0.8 \exp^{-0.5(r_{xy}/\sigma^2)^\gamma} \\ r_{xy} &= (x - x_{\text{off}})^2 + (y - y_{\text{off}})^2, \end{aligned}$$

where x and y are coordinates in the image, and $\text{Bin}(\cdot|n, p)$ is the binomial distribution.

Model parameters are x_{off} and y_{off} , which respectively determine the horizontal and the vertical offset of the blob, γ , defining its contrast, and σ^2 , determining the width width.

For our experiments, we use images of size 32×32 pixels. We choose uniform priors in the range $[-16, 16]$ for x_{off} and y_{off} , and a uniform prior in the range $[0.25, 5]$ for γ . We fix σ to 2.

B.2 Evaluation

We evaluate different acquisition methods by keeping track of the log-likelihood of a test set consisting of 100 parameters-image pairs over the course of acquisitions (starting from an initial sample of size $t_0 = 30$). In addition, we provide posterior predictive checks for an amortized emulator after acquiring $t = 1000$ samples.

B.3 Network architecture and training

Emulator networks model a binomial distribution as output. Neural networks have two hidden layers (200 units each) with ReLu activation functions. We train an ensemble of $M = 25$ networks using Adam [1] with default parameters ($\beta_1 = 0.9, \beta_2 = 0.999$) for SGD with a learning rate of 0.001.

References

[1] D Kingma and J Ba. Adam: A Method for Stochastic Optimization. In *ICLR*, 2015.

C Hodgkin-Huxley example

D Model

The dynamic equations describing the evolution of the membrane potential and of the gating variables of the neuron are taken from [1]:

$$\begin{aligned} C_m \dot{V} &= -(I_{\text{leak}} + I_{\text{Na}} + I_{\text{K}} + I_{\text{M}} + I_{\text{ext}}) \\ &= g_{\text{leak}}(E_{\text{leak}} - V) + \bar{g}_{\text{Na}} m^3 h (E_{\text{Na}} - V) + \\ &\quad + \bar{g}_{\text{K}} n^4 (E_{\text{K}} - V) + \bar{g}_{\text{M}} p (E_{\text{K}} - V) + I_{\text{in}}(t), \end{aligned}$$

where C_m is membrane capacitance, V the membrane potential, I_c are ionic currents ($c = \{\text{Na}, \text{K}, \text{M}\}$) and $I_{\text{in}}(t)$ is an externally applied current which we can imagine as the sum of a static bias I_{bias} and a time-varying zero-mean noise signal $\varepsilon(t)$. I_{Na} and I_{K} shape the up- and down-stroke phases of the action potential (spike), I_{M} is responsible for spike-frequency adaptation, and I_{leak} is a leak current describing the passive properties of the cell membrane. Each current is in turn expressed as the product of a maximum conductance (\bar{g}_c) and the voltage difference between the membrane potential and the reversal potential for that current (E_c), possibly modulated by zero or more ‘gating’ variables (m, h, n, p).

Each $x \in \{m, h, n, p\}$ evolves according to first order kinetics in the form:

$$\dot{x} = \frac{1}{\tau_x(V)} (x_{\infty}(V) - x)$$

We provide a step current as input.

In our example application, free model parameters are g_{Na} and g_{K} . We model uniform priors over these parameters: \bar{g}_{Na} is between 0.5 and 60 and \bar{g}_{K} is between 0.5 and 10.

D.1 Evaluation

We evaluate the posterior obtained through the emulator after $t = 250$ acquisitions, starting from an initial sample size $t_0 = 30$. As posterior predictive check, we span a grid over the parameter space and compare simulator outputs to the posterior.

D.2 Network architecture and training

Emulator networks model a multinoulli (categorical) distribution with $K = 6$ classes as output. Neural networks have two hidden layer (200 units each) with a ReLu activation functions. We train an ensemble of $M = 25$ networks using Adam [1] with default parameters ($\beta_1 = 0.9, \beta_2 = 0.999$) for SGD with a learning rate of 0.001.

References

- [1] M Pospischil, M Toledo-Rodriguez, C Monier, Z Piwkowska, T Bal, Y Frégnac, H Markram, and A Destexhe. Minimal hodgkin-huxley type models for different classes of cortical and thalamic neurons. *Biol Cybern*, 99(4-5), 2008.
- [2] D Kingma and J Ba. Adam: A Method for Stochastic Optimization. In *ICLR*, 2015.

E BOLFI convergence

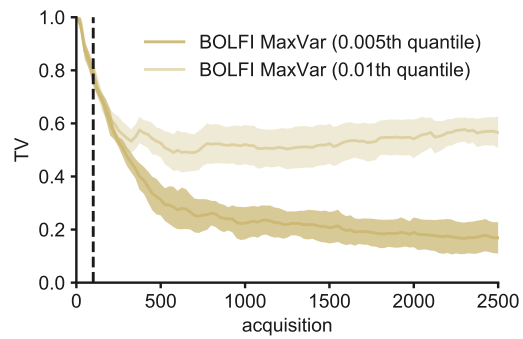


Figure 5: **Convergence of BOLFI *MaxVar*.** In the manuscript, we show performance up to 100 acquisitions. With additional acquisitions, BOLFI also converges. However, the quality of the inferred posterior strongly depends on the value of the threshold parameter used in BOLFI: When the threshold is set adaptively to the 0.01th quantile of realised discrepancies (default choice specified in their paper), performance is markedly worse than when set to the 0.005th quantile.

F *MaxInf* acquisition for Hodgkin-Huxley model

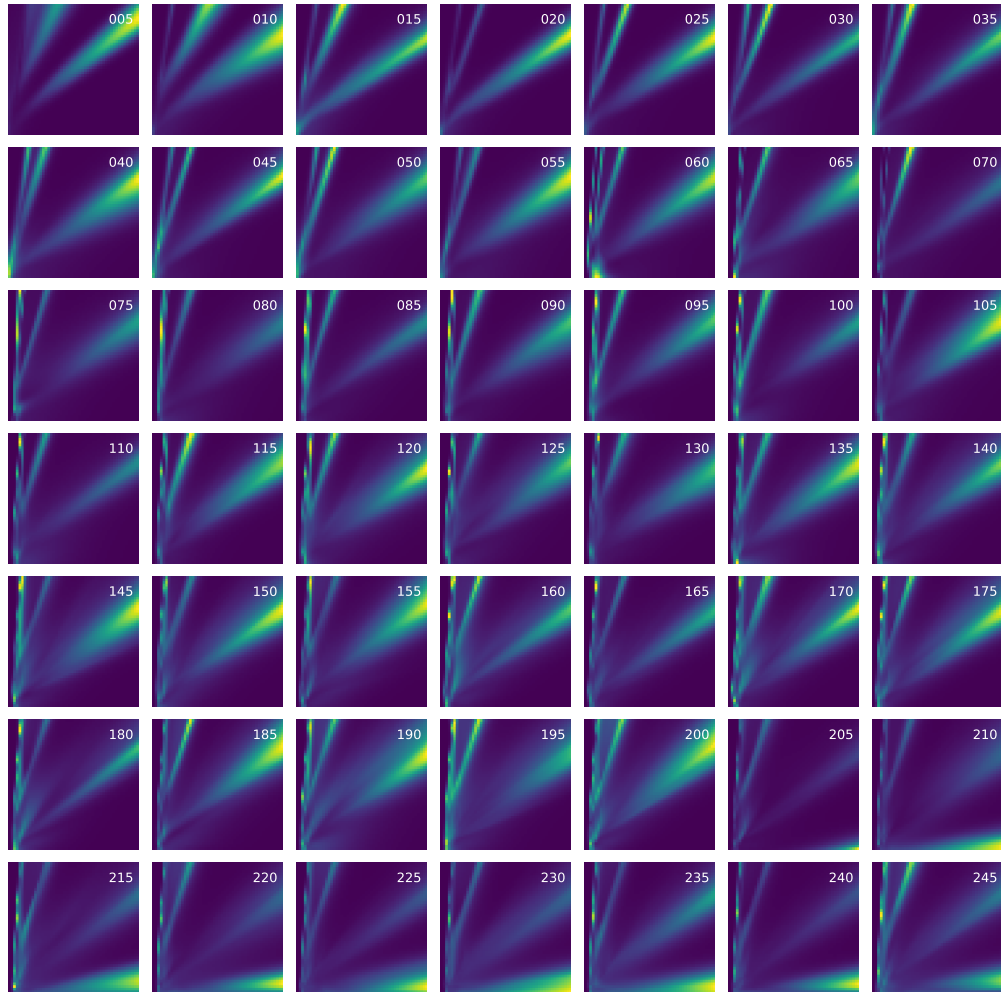


Figure 6: **Acquisition surface for *MaxInf* rule on Hodgkin-Huxley example.** Individual panels show the acquisition surface over θ as additional samples have been acquired. The acquisition rule proposes datapoints at the decision boundaries of the posterior (cf. Fig. 4, manuscript).